A Fe_xMn_{1-x}/Ir(001) multilayer probed by EXAFS and DAFS

S. Grenier,[a]* H. Renevier,[a] J. M. Tonnerre[a] and H. Fischer[b]

[a]Laboratoire de Cristallographie, C.N.R.S., B.P. 166, 38042 Grenoble Cedex 09, France, and [b]Laboratoire de Physique des Matériaux, UHR 7556, CNRS-Université de Nancy, 54006 Vandoeuvre, France. E-mail: grenier@polycnrs-gre.fr

Diffraction Anomalous Fine Structure (DAFS) and EXAFS measurements have been performed on a $[Fe_{0.7}Mn_{0.3}/Ir(100)]_{40}$ superlattice at the K-edges of Fe and Mn. Theoretical EXAFS spectra have been refined: a slight difference in the first neighbor distance suggests a non homogeneous distribution of the Mn in the alloy. The smooth features of the DAFS spectra have been modeled to study the composition and the strain profile along the growth axis.

Keywords: EXAFS; **DAFS**; **superlattice.**

1. Introduction

3d metals are intensively studied for the strong relationship between their magnetic and structural properties that can provide "artificial" materials for designing novel magnetic devices. Mn and Fe have been studied on their moment-volume instabilities, for example the antiferromagnetic Fe and Mn fcc phases are predicted to be ferromagnetic beyond a critical value of the cell volume (Moruzzi, 1999). Fe_xMn_{1-x} alloys have been grown epitaxially on Ir substrates to obtain a larger in-plane lattice parameter and, assuming a homogeneous alloy, to push them into the ferromagnetic phase. However a recent study (Ardhuin, 1998) on a $[Fe_{0.7}Mn_{0.3}/Ir(100)]_{40}$ superlattice (SL) by High Resolution Electron Microscopy and Electron Energy Loss Spectroscopy reports a slight Mn segregation from $1-x=0.25$ to 0.4, with an increase of the Fe magnetic moment along the growth direction. Despite this surfactant effect, the conservation of a single FeMn lattice is observed.

We have studied this same SL by EXAFS in order to get the mean first neighbor distances around Fe and Mn. The DAFS method gives access to details on the structure around the absorber analysing the EXAFS-like oscillations (Proietti, 1999). It also provides information on the electronic configuration of the absorber. Furthermore, we can identify the signal of the anomalous elements located in different crystallographic sites because each one gives a different contribution to the amplitude and the phase of the structure factor. We report in section 4 on the preliminary DAFS study of strain and composition profile of a $[Fe_{0.7}Mn_{0.3}/Ir(100)]_{40}$ SL.

2. Experimental

The SL of 40 bilayers was grown onto an Ir substrate by Molecular Beam Epitaxy, at 400K after growing a MgO buffer. Specular diffraction analysis shows that each bilayer contains about 12 ± 1 planes of the FeMn alloy and 17 ± 1 planes of Ir; its dimension is found to be about 52Å.

Measurements were carried out at the French Cooperative Research Group "D2AM" bending magnet beamline (Ferrer, 1998) at the European Synchrotron Radiation Facility, using a Si(111) monochromator with an energy resolution about 1 eV.

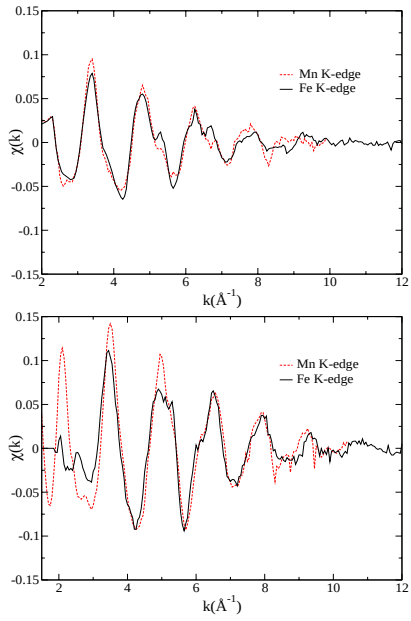

Figure 1
EXAFS with the polarisation parallel (upper panel) and perpendicular (lower panel) to the growth axis.

EXAFS and DAFS spectra were recorded at the K-edges of Fe and Mn at room temperature. EXAFS spectra were recorded using a Silicon photodiode in the fluorescence mode. DAFS spectra were obtained by tracking the maximum of the Bragg peak as a function of the energy through the absorption edge, using a photodiode or a photomultiplier for the weakest peak.

3. EXAFS analysis

EXAFS spectra were recorded for the two elements in geometries with the X-ray polarisation parallel and perpendicular to the growth axis, in order to enhance the signals from in-plane and out-of-plane distances respectively. The oscillations were extracted using AUTOBK (Newville, 1993) (Figure 1) considering the Fermi energy as the first maximum of the derivative as usual for 3d elements. For Mn (Z=25) the spectrum was limited to 10 Å^{-1} due to the presence of the iron edge (Z=26), for Fe the signal doesn't extend after 12 Å^{-1} as it is often observed in such material. The spectra show similar features for the two elements in both polarisation directions.

We performed a multishell analysis of the EXAFS oscillations using *ab initio* phases and amplitudes calculated by FEFF code (Rehr, 1991). Theoretical calculations are based on a self-consistent potential calculated in the muffin-tin approximation. The same starting structure model was used for both elements, i.e. a bct structure with a=2.715Åand c=3.3Å. The c value was obtained from simulation of the SL diffraction pattern. Data refinement was achieved by FEFFIT program (Newville, 1995). Some parameters were fixed: the numbers of neighbors, the in-plane lattice parameter (fixed to the Ir-Ir bulk distance according to Ardhuin (Ardhuin, 1989)) and the Fermi energy fixed to 0.

At the Fe edge, the refinement includes three neighbor distances (single scattering) and three distances corresponding to multi-scattering and focusing effects. Best fits for Fe are presented in

Figure 3; the results for the first shell distance (from absorber to the central atom in the bct cell) are presented in Table 1. It is found

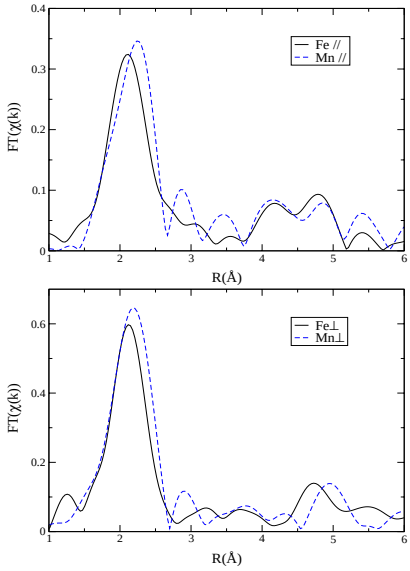

Figure 2
Fourier transform of the EXAFS of Fe and Mn, polarisation parallel and perpendicular to the growth axis.

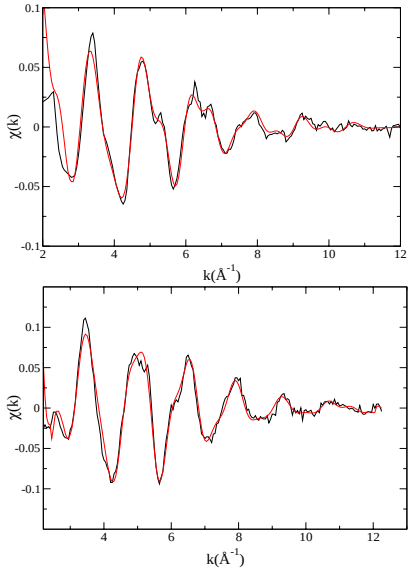

Figure 3
Best refinement for Fe K edge, for parallel (upper panel) and perpendicular (lower panel) polarisation.

to be very close to the initial model, with a tetragonality ratio of c/a = 1.21.

The slight differences between Fe and Mn could been explained by a different mean position in the layer. However in the case of the Mn only the first shell has been refined because of refinement unstabilities for the next nearest neighbor environment. Fixing the first Mn-Mn distance at 2.58Å, the structure of Mn atoms should be bct with $c \approx 3.44$Åand with a tetragonality ratio of 1.27 as already found for the FeMn alloy by Ardhuin.

Table 1
EXAFS multishell fits results for the parallel and perpendicular polarisations

First neighbor distances Å	σ^2 Å^2
Fe // 2.526 ± 0.02	0.010
Fe // 2.526 ± 0.02	0.010
Fe $\perp$ 2.53 ± 0.02	0.008
Mn // 2.58 ± 0.02	0.014
Mn $\perp$ 2.54 ± 0.02	0.009

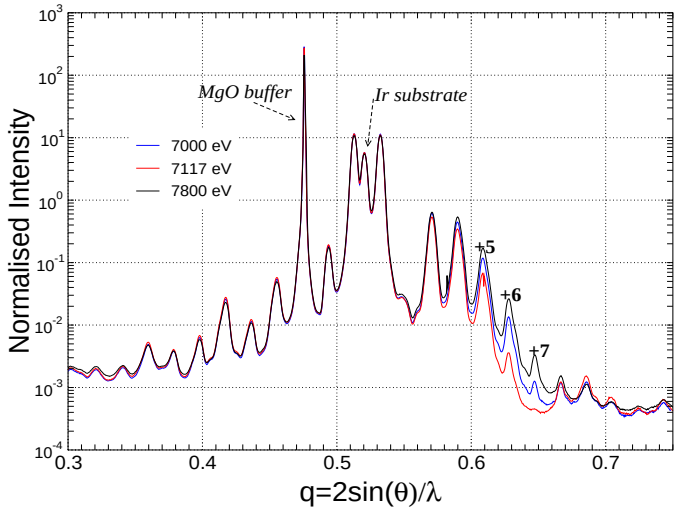

Figure 4
Diffraction pattern of the multilayer at 3 energies aound the Fe K-edge (7000 KeV, 7117 KeV and 7800 KeV).

4. DAFS analysis

For a multilayer the diffraction pattern with $\vec{q}$ along the growth axis contains numerous Bragg peaks due to the large vertical dimension of the periodic cell (52.14Å). We have measured diffraction spectra at three energies around each absorption edge to see the trend of the anomalous effect on each peak. Figure 4 shows that around the Fe K-edge, only three peaks are of particular interest (noted +5, +6 and +7, in reference to the substrate peak). This is due to the high contribution of the Ir atoms to the diffraction pattern. The DAFS spectra of the three peaks are displayed in Figure 5.

Without taking into account the fine structure, the smooth behaviour of the diffraction peak can be refined using the formula (eq.1):

$$|F_0|^2 = |F_T|^2 \left(\left(\cos(\Delta\varphi) + \beta f' \right)^2 + \left(\sin(\Delta\varphi) + \beta f'' \right)^2 \right)$$

where $F_T = |F_T| \exp(i\varphi_T)$ is the structure factor including all the non anomalous terms, $\Delta\varphi = \varphi_T - \varphi_A$, φ_A being the phase of the geometrical term including the anomalous atoms only and $\beta = \left| \frac{\sum c_i \exp\left(i2\pi \vec{q} \cdot \vec{r_i}\right)}{F_T} \right|$, with c_i the concentration of the anomalous atom on the plane i. The refinement of the DAFS spectra showed that no distortions are observed in the whole energy range.

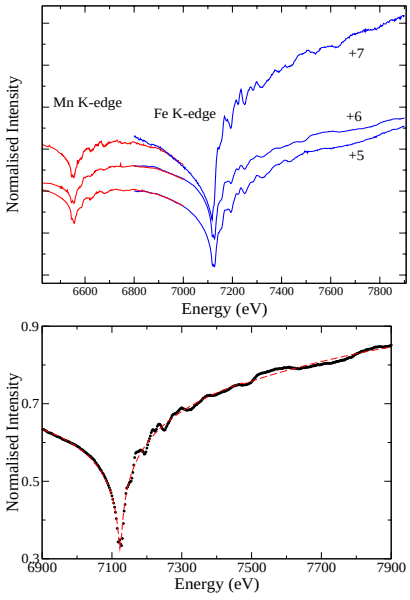

Figure 5
(upper panel) DAFS on +5, +6 and +7, the Mn and Fe spectra have been linked perfectly for +5 and +6 but not for +7. The peaks have been rescaled for presentation. (lower panel) Refinement with eq. 1, showing no distorsion of the peak.

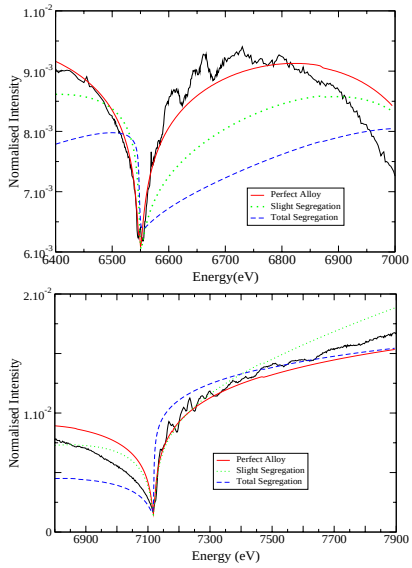

Figure 6
Calculation of diffracted intensity for three composition profile, on peak +7.

The ratio of β of each element at each peak gives a hint for the layer composition in case of a perfect alloy. It gives 0.47(4) and 0.42(5) for the peak +5 and +6: close to the nominal stoichiometric ratio 3/7(=0.43). This ratio is 0.35 for the +7 satellite, although this result has to be confirmed improving data quality (the spectra at the two edges did not match well to each other despite of background correction for fluorescence and diffuse scattering).

The diffracted intensity from a crystallographic model has been calculated. Three models have been tested with different out of plane parameters and different composition profile: a perfect alloy, a layer with a slight segregation (0.2 to 0.4 along the growth axis) and also a total segregation (4 Mn planes at the top of the layer). The anomalous terms are calculated from Cromer Liberman tables. The formula $s * (pE + 1)\,|F|^2 + cst$ has been refined, where s is a scale factor, p describes a detector factor and cst an *ad hoc* constant. The current results and analysis are still prelimary, however we found that the +7 peak is the most sensitive to the composition profile and the best results are obtained for an out of plane parameter $c = 3.3$ Å. We mean to pursue the study to get a more realistic modeling of the SL, to this end the analysis of the DAFS oscillations will be essential.

5. Conclusion

The first neighbor distance is found to be not the same for Fe and Mn in the $[Fe_{0.7}Mn_{0.3}/Ir(100)]_{40}$ SL. DAFS analysis on this sample is made more complicated by the huge scattering power of Ir. It dominates a large part of the diffraction spectra and only a little interval in q is available, reducing the analysis to Bragg peaks that are very close to each other. Modeling of the diffracted intensity shows that DAFS can still be helpful even in such an unfavorable case. Study of the DAFS oscillations is now in progress.

We acknowledge the staff of the CRG-D2AM beamline, S. Arnaud, B. Caillot and J.F. Brar for technical assistance.

References

Ardhuin H., Suenaga K., Casanove M.J., Snoek E., Colliex C., Fischer H., Andrieu S., Piecuch M., (1998), *Phys. Rev.B*, 14135-14138.
Ferrer J. L., Simon J. P., Bérar J. F., Caillot B., Fanchon E., Kaikati O., Arnaud S., Guidotti M., Pirocchi M. and Roth M., (1998). *J. Synchrotron Rad.* **5**, 1346-1356.
Moruzzi V.L., Marcus P.M. and J. Kobler (1998), *Phys. Rev. B* 39, 6957-6961.
Newville M., Livins P., Yacoby Y., Rehr J.J., Stern E.A. (1993), *Phys. Rev. B* 47, 14126-14131.
Newville M., Ravel B., Haskel D., Rehr J.J., STern E.A. and Yacoby Y, (1995), *Physica B* 208&209, 154-155.
Proietti M.G., Renevier H., Hodeau J.L., Garcia J., Bérar J.F. and Wolfers P. (1999), *Phys. Rev. B*, Vol. 9, No 8, 5479-5492.
Rehr J.J., Mustre de Leon J., Zabinsky S.I., Albers R.C. (1991), *J. Am. Chem. Soc.* **113**, 5135-5139
Stern E.A., Newville M., Ravel B., Yacoby Y. and Haskel D. (1995), *Physica B* 208&209, 117-127.